Measurement of Local Diffusion Coefficients in Biofilms by Microinjection and Confocal Microscopy

Dirk de Beer, Paul Stoodley, and Zbigniew Lewandowski*
Center for Biofilm Engineering, Montana State University, Bozeman, MT 59717

Received January 16, 1996/Accepted May 20, 1996

A new technique for the determination of local diffusion coefficients in biofilms is described. It is based on the microinjection of fluorescent dyes and quantitative analysis of the subsequent plume formation using confocal laser microscopy. The diffusion coefficients of fluorescein (MW 332), TRITC-IgG (MW 150000) and phycoerythrin (MW 240000) were measured in the cell clusters and interstitial voids of a heterogeneous biofilm. The diffusivities measured in the voids were close to the theoretical values in water. Fluorescein had the same diffusivity in cell clusters, voids, and sterile medium. TRITC-IgG did not diffuse in cell clusters, presumably due to binding to the cell cluster matrix. After treatment of the biofilm with bovine serum albumin, binding capacity decreased and the diffusion coefficient could be measured. The diffusivity of phycoerythrin in cell clusters was impeded by 41%, compared to interstitial voids. From the diffusion data of phycoerythrin it was further calculated that the cell cluster matrix had the characteristics of a gel with 0.6 nm thick fibers and pore diameters of 80 nm.

Key words: biofilms • biofilm structure • diffusivity • mass transport in biofilms

INTRODUCTION

Microbial conversions in biofilms are controlled by growth kinetics and mass transport processes. Therefore, direct determination of mass transport resistances in biofilms are necessary for the modeling of substrate conversion rates. Furthermore, mass transport resistance has been cited frequently as the cause of the reduced efficacy of antibiotics, biocides, and antibodies to biofilm cells as compared to suspended cells (Anwar et al., 1992; Griebe et al., 1994; Marrie et al., 1979; Nichols et al., 1989). Conventionally, molecular diffusion is considered the predominant mechanism for solute transport in biofilms. Consequently, internal mass transport is frequently described using a single effective diffusion coefficient (D_e). Numerous studies reporting measurements of the D_e of various compound in biofilms and microbial aggregates have been reviewed (Christensen and Characklis, 1990; Libicki et al., 1988; Siegrist and Guyer, 1985). Literature values show a wide range of variation, D_e being 1%–900% of the diffusion coefficient in water (D_w), reflecting the variety of biofilms studied as well as the different measurement methods. The D_e/D_w ratios for substrates with small molecular weights, such as oxygen, glucose, ammonium, and nitrate, in spontaneously grown biofilms and microbial aggregates are assumed to be around 0.9 (Christensen and Characklis, 1990). Diffusion of macromolecules such as DNA, dextrans, and proteins may be more strongly impeded by biofilm matrices, resulting in decreased D_e/D_w ratios. Diffusion experiments with such molecules have been reported only for gel matrices, however, biofilms can be considered as highly hydrated gels (Christensen and Characklis, 1990). An extensive review on diffusion phenomena in gels is given by Westrin (1991). It has been shown that the D_e/D_w of proteins diffusing through agarose gels is inversely correlated with their molecular weight (Arnold et al., 1985; Boyer and Hsu, 1992). This is due to gel matrix polymers obstructing diffusion (Rodbard and Chranbach, 1970) as well as hydrodynamic drag at the matrix polymer-solvent interface (Brenner and Gaydos, 1977). The impeded diffusion of large molecules in gels is strongly influenced by the microstructure of the gel matrices. Consequently, information about the microstructure of the biofilm matrix may be derived from diffusion data. However, reversible binding of the diffusing compound to the polymer matrix may decrease the diffusivity in gels (Radomsky et al., 1990).

Diffusivities in biofilms have been estimated by measuring transient or steady state fluxes through biofilms in diffusion chambers or in uptake experiments. If the experiments are performed with a nonreacting compound or with killed biofilms, D_e can be calculated by fitting the measured fluxes to a diffusion model. In the case of a reacting compound, a reaction-diffusion model is required.

Recent application of confocal scanning laser microscopy (CSLM) to biofilm research has shown that biofilms can have a complex structure consisting of cell clusters, discrete aggregates of microbial cells in an EPS matrix, and interstitial voids, open channels connected to the bulk liquid (de Beer et al., 1994b; Lawrence et al., 1991; Massol-Deya et al., 1994). It was shown that in voids both convection and diffusion can occur, although in cell clusters molecular diffusion is the sole mechanism responsible for mass transport (de Beer et al., 1994c). The average D_e determined in natu-

* To whom all correspondence should be addressed. Telephone: 406-994-4770; fax: 406-994-6098; e-mail: ZL@erc.montana.edu

CCC 0006-3592/97/020151-08

rally grown biofilms, using the methods described above, may comprise both diffusional and convectional transport. This may explain why D_e values higher than D_w have been reported (Libicki et al., 1988; Siegrist and Gujer, 1985). It is possible that substances, such as biocides, antibiotics, and antibodies, can be transported readily through biofilm voids but cannot penetrate into the cell clusters where the bacteria are localized. For a more complete description of mass transport it is necessary to know the local diffusion coefficients within the biofilm (i.e., in the voids and in the cell clusters).

Local diffusivities have been measured with the fluorescence recovery after photobleaching (FRAP) technique. If FRAP is used with conventional microscopy it is suitable for 2-D diffusion measurements (e.g., mobility of a species in a membrane (Axelrod et al., 1976). FRAP in combination with confocal scanning laser microscopy (CSLM) theoretically enables 3-D diffusion studies (Blonk et al., 1993).

Our goal was to measure diffusion coefficients of various compounds in defined regions of an intact, heterogenous biofilm and, using these data, to describe the microstructure of the biofilm matrix. We developed a method for the measurement of diffusion coefficients by analyzing the plume formation after microinjection of fluorescent dyes. Essentially, the calculations for diffusion coefficients are similar to those necessary for FRAP. However, instead of diffusion into an area depleted of dye, the diffusion of a dye out of an initial spherical plume is followed. The method is straightforward and the numerical procedures are simpler than those used in the FRAP method.

MATERIALS AND METHODS

Biofilm Reactor

The reactor system consisted of a polycarbonate closed channel (0.5 cm wide, 1.0 cm deep) flow cell in a recycle loop which also includes an aeration/mixing chamber. The flow cell had a rectangular glass coverslip viewing port (60 × 24 mm) 15 cm from the inlet. The inlet port was tapered in a 14° angle to minimize entrance effects. The flow cell was connected to the support system with flexible tubing so it could be mounted on a microscope stage. The biofilm developed on the coverslip could be microscopically examined in situ and was accessible for specially designed ''J'' shaped micropipettes (Fig. 1) (de Beer et al., 1994c). The reactor was initially filled with a minimal salts medium (2.2 mM KH_2PO_4, 4 mM K_2PO_4, 0.76 mM $(NH_4)_2SO_4$, 4.1 × 10^{-2} mM MgS_4O, and 2.2 mM glucose, pH 7.0) and inoculated with frozen stock cultures of *Klebsiella pneumonia, Pseudomonas fluorescens and Pseudomonas aeruginosa.* The reactor was run in batch mode for 6 hours to allow colonization of the coverslip and subsequently was switched to continuous culture with a liquid residence time of 26 minutes and recycle flow rate of 4.5 mL/s (U_{avg} = 9.5 cm/s). The biofilm was allowed to develop for 4–5 days before performing the diffusion experiments. All experiments were performed at 20 ± 1°C.

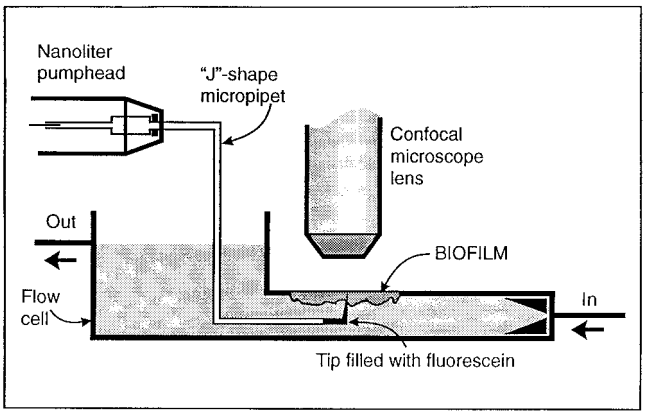

Figure 1. Schematic of the experimental set-up: pumphead with J-shaped micropipet, confocal microscope lens, flow cell, and observation window with biofilm.

Confocal Microscopy

The biofilm structure was visualized using confocal microscopy (Bio-Rad MRC600 attached to an Olympus BH2 light microscope, with 10X or 20X objectives (de Beer et al., 1994b). The biofilm was slightly autofluorescent when excited at 488 nm and could be imaged without staining, avoiding possible interference with the dyes used for diffusion analysis. Image analysis was performed using the Bio-Rad COMOS software. The void fraction (or surface coverage) of the biofilm was measured using a thresholding technique in which the threshold was adjusted manually until the biofilm clusters were white and the surrounding voids black. The software then returned the proportion of black to white areas.

Microinjection Technique

The local diffusion coefficients in cell clusters and voids were determined by injecting small volumes of fluorescent dye. A nanoliter pump (Model A1400 World Precision Instruments [WPI], Sarasota, FL), with a ''J'' shaped micropipet was used to inject dye into the biofilm. The micropipet was made by first pulling a glass capillary (1 mm, 1B100-4, WPI) to a microtip of 5–10 μm, and then bending it 90° at 4 mm and 45 mm from the tip to form the ''J''-shape. The micropipet was filled with mineral oil and connected to the pumphead. The tip was filled by dipping it into the dye solution and running the pump in reverse. Special care was taken to avoid the inclusion of air bubbles inside the pipet. The pumphead with the micropipet was mounted on a micromanipulator (Model M3300R WPI) with a stepper motor (Model 18503 Oriel, Stratford, CT) to enable positioning with 1 μm accuracy. The tip was positioned inside a cell cluster or void using the micromanipulator under microscopic observation. Exact positioning of the tip in the focal

plane was performed using the CSLM. The pump rate was set at 0.1 nl/s and the injection time was 1 second. The pulses were delivered by positioning the tip 500 μm below the focal plane, switching the pump on, moving the micropipet into the focal plane, removing it after 1 second, and then switching off the pump. The velocity of the micromanipulator was 500 μm/s.

To avoid convection in the reactor the recycle pumps were turned off for a few minutes before dye injection into the cell clusters and the voids. However, to measure the diffusion coefficient of fluorescein in sterile medium, the reactor had to be left overnight to obtain complete stagnancy. The diffusion coefficient of IgG TRITC conjugate and phycoerythrin could not be measured in sterile medium because the tip of the micropipet plugged in the time required to achieve complete stagnation.

Fluorecent Dyes

Three dyes were used in the experiments: 1) fluorescein (Sigma, St. Louis, MO); 2) antimouse IgG (whole molecule) TRITC conjugate (2 g/l, Sigma, St. Louis, MO); 3) R-phycoerythrin (4 g/l, Molecular Probes, Eugene, OR) prepared as instructed in 0.1 M sodium phosphate and 0.1 M sodium chloride.

TRITC conjugated IgG was also tested after bovine serum albumin (fraction V, Sigma, St Louis MO) was added to the reactor to achieve final concentration of 20 g/l and allowed to incubate for 30 minutes.

Factors Influencing Fluorescence

The relationship between the dye concentration in the minimal salts medium and its fluorescent intensity was measured from CSLM images of the liquid. To avoid differences due to light extinction with depth, the images were captured at the same focal plane, just below the liquid/air interface where a maximum intensity was reached. This depth was found from sectioning through the air/liquid interface into the liquid. The average fluorescent intensities of the full images (768 × 512 pixels) were measured. The settings of the CSLM were the same for all the dye concentrations tested.

The rate of photobleaching was evaluated by subjecting a polycarbonate membrane filter (0.2 μm; Poretics, Livermore, CA) soaked wtih the dye to different laser intensities, and recording the average fluorescent intensity of the full image during 1 minute. To avoid complications, the laser intensity during the diffusion measurements was adjusted so that photobleaching was negligible.

The fluorescence of fluorescein in the cell clusters was found to be less intense than in the void areas, possibly because of quenching by EPS. To estimate the extent of EPS quenching, the fluorescence intensity of each of the dyes dissolved in various concentrations of kelp alginate (sodium salt, low viscosity, Sigma A 2158, St Louis, MO) was measured. Alginate was used because it is an important constituent of biofilm EPS and has been well-described in the literature (Christensen and Characklis, 1990; Siebel and Characklis, 1991).

Determination of Diffusion Coefficients

Sequences of images of the fluorescent plume developing around the micropipet tip were recorded at equal time intervals. The average fluorescence intensity of a 9 × 6 pixel box was recorded at a defined radial distance from the point of origin for each of the images in the sequence. Subsequently, the peak time (the time between pulse delivery and maximal fluorescent intensity) was determined. The distribution of a substance diffusing from an instantaneous spherical source in an infinite medium is described by the equation (Crank, 1975):

$$C_r = \frac{1}{2} C_0 \left(erf \frac{a+r}{2\sqrt{Dt}} + erf \frac{a-r}{2\sqrt{Dt}} \right) - \frac{C_0}{r} \sqrt{\frac{Dt}{\pi}} \left(e^{-(a-r)^2/4Dt} - e^{-(a+r)^2/4Dt} \right). \quad (1)$$

The diffusion coefficient can then be found by reiterative curve fitting so that it is consistent with the measured peak time at the known radial distance.

Estimation of Microstructure from Diffusion Data

We used the diffusion data from phycoerythrin to obtain structural information about the cell cluster matrix. Phycoerythrins are light-harvesting molecules in algae and have evolved to maximize absorbance and fluorescence, the water-soluble proteins do not bind nonspecifically to cells (Glazer, 1988). These properties make it an excellent compound to study purely diffusional phenomena of large molecules.

If the cell cluster matrix is considered a porous solid medium, the impedance of the matrix is determined by the porosity and tortuosity:

$$\frac{D_e}{D_w} = \frac{\epsilon}{\tau^2} \quad (2)$$

The value for ϵ/τ^2 can be determined with a nonreacting, low MW tracer, such as ^3H_2O (Rudd et al., 1986). In this study we used fluorescein as the tracer. It has been shown that D_e/D_w in gels also depends on the MW of the diffusing compound (Arnold et al., 1985; Boyer and Hsu, 1992). Consequently, Eq. 2 does not give a general relation between matrix structure and diffusion phenomena for both small and large molecules. For large molecules the molecular radius of the diffusing compound and the pore size of the matrix have to be taken into account, which is expressed in the modified Renkin equation (Satterfield et al., 1973).

$$\frac{D_e}{D_W} = \left(\frac{1-\varphi_p}{\tau^2}\right)\left(1-\frac{R^a}{R_p}\right)^2 \left(1-2.104\frac{R_a}{R_p}+2.09\left(\frac{R^a}{R^p}\right)^3-0.956\left(\frac{R^a}{R^p}\right)^5\right). \quad (3)$$

With Eq. 3, R_p of the cell clusters was calculated from measured diffusion data. R_a was calculated from the measured diffusion coefficient in medium using the Stokes–Einstein relation:

$$D_W = \frac{k_B T}{6\pi\eta R_a}. \quad (4)$$

The thickness of the polymer fibers was estimated using Ogstens theory for hindered diffusion (Muhr and Blanshard, 1982):

$$\frac{D_e}{D_W} = e^{-\varphi_p^{0.5}\left(\frac{R_a+R_f}{R_f}\right)}. \quad (5)$$

RESULTS

The biofilms consisted of cell clusters attached to the substratum, separated by voids. The thickness of the cell clusters was 150–200 μm and their width was 150–300 μm. The void fraction was approximately 50%.

Factors Affecting Fluorescence

The fluorescence intensity of fluorescein in medium was not linear with concentration (Fig. 2a), but had a maximum at about 2 mM. Additionally, fluorescence intensity was decreased by alginate with a 50% reduction at a concentration of 2% (Fig. 2b). Quenching by alginate was the same for 0.01 and 2 mM fluorescein. The optical density of the alginate solutions, measured at 488, 560, and 668 nm, differed less than 1% from water. Since the alginate concentration in the biofilms was unknown and because of the nonlinearity of the fluorescence intensity with the dye concentration, the fluorescence intensity was not considered a reliable indication for the local fluorescein concentration. However, below a concentration of 2 m*M* the fluorescence intensity was positively correlated to the dye concentration. Therefore, the peak in fluorescence intensity, at a defined radial distance from the micropipet tip, corresponded to the maximum fluorescein concentration. The fluorescence intensity of TRITC-IgG was proportional to the concentration and no quenching by alginate was observed (data not shown). Fluorescence intensity of phycoerythrin was also proportional to concentration, but was quenched by 75% in a 3% alginate solution (data not shown).

Measured Diffusion Coefficients

After a pulse injection of fluorescein or phycoerythrin in the voids or cell clusters, the fluorescent plume expanded away from the micropipet tip. As it expanded it simultaneously faded in intensity, due to dilution of the dye, until background levels were reached (Fig. 3). The diameter of the

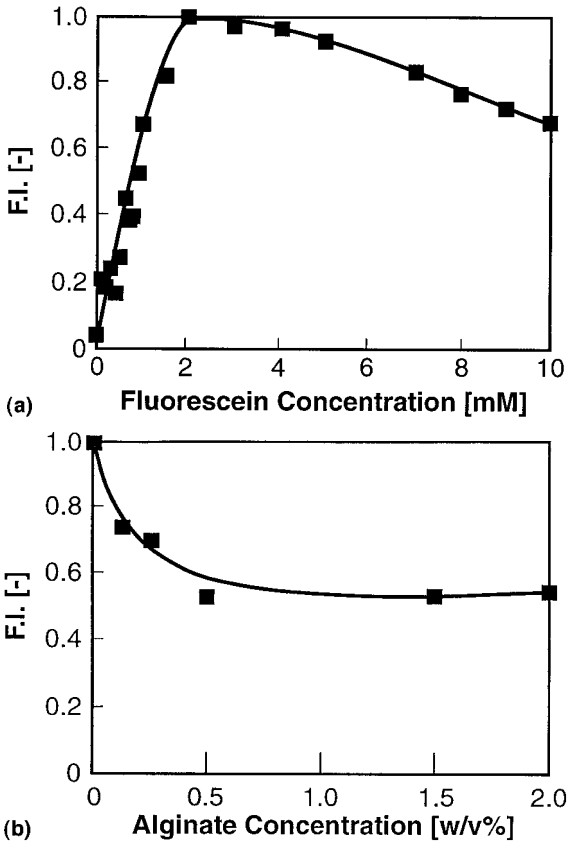

Figure 2. The fluorescence intensity (FI, expressed as $FI/FI_{(max)}$) of fluorescein was not linearly related to fluorescein (A) or alginate concentration (B).

initial plume was usually about 20 μm, corresponding to a volume of 3.4×10^{-2} nl. The volume of the injected dye was at least three orders of magnitude smaller than the volume of the cell clusters and probably had negligible effects on the cell cluster structure. The same was observed upon injection of TRITC-IgG into voids, however, in the cell clusters the plume expanded only slightly and did not fade. Consequently, peak times could not be measured. After pretreatment with bovine serum albumin (2%, 30 minutes) injection of TRITC-IgG resulted in an expanding plume of decreasing fluorescence intensity, similar to the observations with fluorescein and phycoerythrin. Although the fluorescent intensity did not decrease to background levels, peak times could be recorded.

An example of the observed fluorescence intensity at a defined distance from the point of origin and the calculations using Eq. 1 is shown in Figure 4. Estimated values of diffusion coefficients in voids, cell clusters and sterile medium are presented in Table 1.

Information on the microstructure of the cell clusters was calculated from the phycoerythrin diffusion data. The polymer volume fraction (φ_p) was assumed to be 0.04, with a corresponding value for the porosity of the matrix (ϵ) of 0.96 (Christensen and Characklis, 1990). Because the fluorescein diffusion was almost unaffected by the biofilm matrix, the tortuosity was close to unity (1.02). The molecular

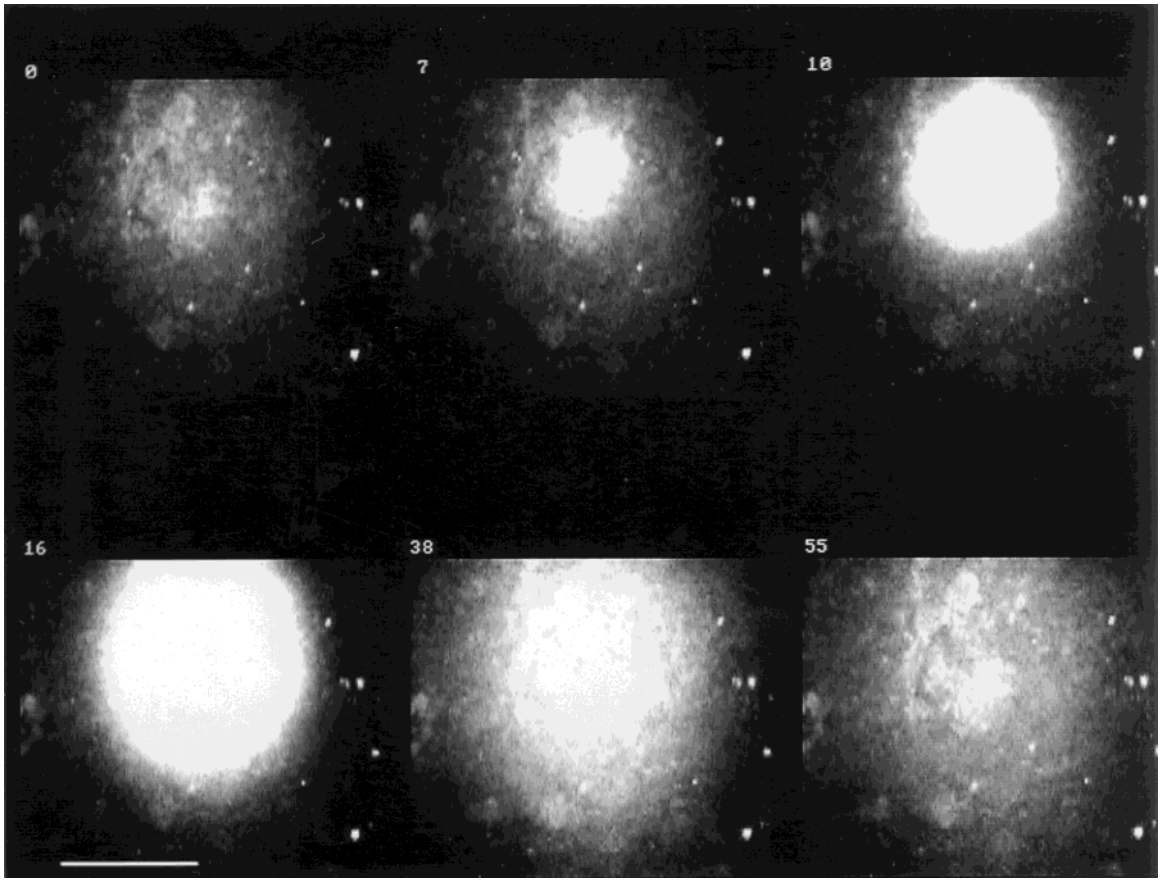

Figure 3. The expansion and dissipation of a fluorescent plume after a pulse injection of fluorescein dye monitored with confocal microscopy. The diffusion coefficient was calculated from the time taken for a concentration wavefront to reach a known distance from the origin. Images were taken at the indicated times (s) after injection. Scale bar = 250 μm.

radius of phycoerythrin was calculated, using Eq. 4, to be 5.5 nm. From these data and the D_e/D_w ratio of phycoerythrin, using Eq. 3, a pore diameter of 80 nm was calculated. According to Eq. 5, the thickness of the polymer fibers was 0.6 nm.

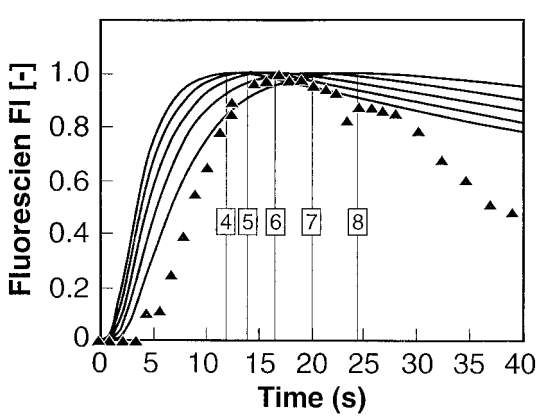

Figure 4. Measured fluorescence intensity (▲, FI, expressed as $FI/FI_{(max)}$) and calculated concentrations (–, C, expressed as $C/C_{(max)}$) of fluorescein at a radius of 140 μm from the tip of the microcapillary after dye injection. The solid vertical lines indicate the peak times for each calculation, the numbers in the boxes represent the various values of D ($\times 10^{10}$ m^2/s) for the various peak times.

Calculated Diffusion Coefficients

The theoretical diffusion coefficients of the dyes was calculated for comparison with the measured values. The theoretical molecular diffusion coefficient of fluorescein in water calculated with the Wilke–Chang method (Treybal, 1981) is 0.48×10^{-9} m^2/s. This value is very close to our measured values in sterile medium (0.55×10^{-9} m^2/s) and voids (0.6×10^{-9} m^2/s). The measured values were also similar to reported values at 25°C (0.5×10^{-9} m^2/s (Berg, 1983; Nugent and Jain; 1984); 0.55×10^{-9} m^2/s) (Rodomsky et al., 1990), indicating that microinjection is a reliable technique for the determination of local diffusion coefficients.

For the larger phycoerythrin and TRITC-IgG molecules an empirical equation was used to find the D_w (Young et al., 1980):

$$D_W = 8.34 \times 10^{-12} \left(\frac{T}{\eta MW^{1/3}} \right) \qquad (6)$$

The reported average error of Eq. 6 is 19% for proteins with MW ranging from 16,890 to 225,000 (Boyer and Hsu, 1992). The calculated D_w, according to Eq. 6, for IgG was 4.6×10^{-11} m^2/s, 29% below the value measured in voids

Table I. Diffusion coefficients (D) for fluorescein, TRITC-IgG, and phycoerythrin at different locations in the biofilm.*

Dye	MW	Injection location	$D \times 10^{-10}$ (m^2/s)	D_c/D_v
Fluorescein	332	Sterile medium	5.5 (± 0.4)	—
		Biofilm void	6.0 (± 0.8)	—
		Cell cluster	5.8 (± 1.0)	0.97
TRITC-IgG	150K	Biofilm void	0.65 (± 0.07)	—
		Cell cluster	0	0
		Cell cluster after 30 minutes exposure to 2% BSA	0.20 (± 0.03)	0.31
Phycoerythrin	240K	Biofilm void	0.39 (± 0.04)	—
		Cell cluster	0.23 (± 0.03)	0.59

*D_c/D_v is the ratio of the measured diffusion coefficients in cell clusters and voids.

and for phycoerythrin 3.9×10^{-11} m^2/s, which was equal to the measured value in voids.

DISCUSSION

Quantitative analyses of the fluorescent plumes developed upon microinjection allowed determination of local diffusion coefficients in biofilm voids and clusters.

It was not possible to give a pulse injection with a stationary pipet because of the slow response time of the pumping system. Either the plume appeared after a few seconds delay or dye continued to be dispensed after the pump was switched off. Either flaw will result in underestimation of the diffusion coefficient. This was possibly caused by compressability in the system; from microscopic air bubbles in the tubing, the elasticity of the tubing, or the dye itself. With the method using a moving pipet, while continuously pumping dye, these problems were avoided. A greater concern was that the movement of the microelectrode and the pumping of the dye may induce convection currents in the dye and surrounding liquid resulting in the overestimation of the diffusion coefficient. Another assumption was that the dye plume was spherical but because we observed the plume expand in one plane only, we could not verify this. We could observe dispersion in the plane perpendicular to the dye injection but not in the plane parallel with the dye injection. It is probable that effects such as these resulted in the differences between the observed data curve and the family of curves predicted from the diffusion model shown in Figure 4. However, the calculated diffusion coefficient for fluorescein in sterile media using this technique was similar to the theoretical value in water and other measured values using different techniques. Although we also tried to measure the diffusion coefficients of IgG and phycoerythrin in sterile media, for controls, we had problems maintaining convection-free liquid. The design of a stagnation chamber that could be viewed microscopically and allow microelectrode access may be difficult but is necessary to validate the technique for other dyes and more extensive transport studies.

The method with the moving pipet was also used for the experiments with TRITC-IgG and phycoerythrin.

The measured diffusion coefficients of fluorescein in cell clusters and voids were very close. Therefore, it was concluded that the diffusivities of nonbinding compounds with molecular weights comparable to that of fluorescein are not significantly decreased in cell clusters. Many nutrients, as well as biocides and antibiotics, have molecular weights of the same order of magnitude or less, as that of fluorescein. This implies that the strongly reduced efficacy of antibiotics and biocides against biofilms can not necessarily be explained by the diffusion resistance of the matrix for these compounds as hypothesized previously (Costerton et al., 1987). The reduced efficacy of chemical challenges to biofilm bound cells must be due to other mechanisms, such as binding or neutralization of the biocidal compounds in the biofilm matrix (de Beer et al., 1994a), or physiological differences between biofilm cells and suspended cells (Brown et al., 1988; Eng et al., 1991; Nichols et al., 1989).

The diffusion of large molecules is impeded by the cell cluster matrix, as indicated by the D_e/D_w ratio of TRITC-IgG and phycoerythrin. The cell cluster matrix can reduce the diffusivity of large molecules in at least two ways: (1) by physical obstruction or (2) by molecular binding. TRITC-IgG diffusion is much more strongly impeded than phycoerythrin, although it is a smaller protein. The diffusion coefficient seemed to be strongly reduced by nonspecific binding of the TRITC-IgG with the cell cluster matrix. Initially no diffusion could be detected at all in cell clusters, since all of the injected TRITC-IgG was apparently bound to the cells or polysaccharide matrix. However, after exposure of the biofilm to BSA, IgG did diffuse, presumably because BSA blocked a part of the binding sites. The D_e/D_w ratio of TRITC-IgG in cell clusters in BSA treated biofilms was close to the value of 0.32 reported for mucus material (Radomsky et al., 1990).

From Eq. 4, using the measured D_w for phycoerythrin, a value for R_a of 5.5 nm was calculated, thus the pore diameter of the cell cluster matrix must be at least 10 nm to allow diffusion of phycoerythrin. A previous study showed that 300 nm BSA treated latex beads do not penetrate cell clusters (de Beer et al., 1994b). Consequently, the pore diameter of the cell cluster matrix is between 10 and 300 nm.

By applying Eqs. 2–5 on the diffusion data and molecular size of phycoerythrin a more precise description of the matrix was obtained. The tortuosity in cell clusters, calculated with Eq. 2, for phycoerythrin and fluorescein was 1.26 and 1.02, respectively. Since the matrix structure is not influenced by the diffusing compounds, Eq. 2 cannot be used to describe diffusion phenomena for both large and small molecules in cell clusters. The diffusion data of phycoerythrin revealed that the biofilm had the characteristics of a gel with a pore diameter of 80 nm (calculated using Eq. 4) and fibers 0.6 nm thick (calculated using Eq. 5). This suggests that only particles smaller than 80 nm can diffuse through the cell cluster matrix, although bigger particles, such as cells, are entrapped. This calculated value of the biofilm matrix pore diameter is within the limits of 11 and 300 nm as estimated from the diameters of phycoerythrin and latex beads. For agarose gels, a pore diameter of 300 nm and a fiber diameter of 3–6 nm is reported (Waki et al., 1982).

The theoretical diffusivity of IgG in cell clusters was calculated assuming the above-described gel structure that would only physically obstruct diffusion. Using Eq. 3 and Eq. 4, a D_e/D_w ratio of 0.7 was calculated. In untreated biofilms this ratio was 0, after BSA treatment 0.7. This shows that the IgG diffusion is influenced much more by binding to bacterial cells and matrix polymers than by physical obstruction, even in BSA-treated biofilms. It should be emphasized that with the technique of microinjection the diffusion coefficient is measured under transient conditions. This may be different from the diffusion of substrates and products under steady state conditions, when the rate of substrate transport into the biofilm is equal to the conversion rate. Binding is inherently a transient process. Only after binding has stopped (when binding is in equilibrium with dissociation or when all binding sites are occupied) steady state is possible, during which no further binding occurs. Consequently, transient state measurements underestimate the diffusion coefficients for steady state transport if the compound can bind to the matrix (Libicki et al., 1988).

Eqs. 3 and 5 are based on several simplifying assumptions and can give only a rough indication of the cell cluster matrix microstructure. More detailed studies on transport phenomena of compounds with different sizes, shapes, and binding properties are needed, as well as measurements in other types of biofilms. Such studies, combined with examinations using TEM and SEM focused on the visualization of EPS fibers, will permit a better insight in the relation between the biofilm microstructure and transport phenomena.

CONCLUSIONS

The resistance of the biofilm cell cluster matrix to diffusion of fluorescein, a small nonbinding molecule, is negligible. The diffusion coefficient of phycoerythrin (MW 240000) in cell clusters was 41% less than in biofilm voids. The measured impedance of phycoerythrin diffusivity indicates that the microstructure of cell clusters was equivalent to a polymer gel consisting of fibers, 0.6 nm thick, forming a network with pores of 80 nm diameter. The reduced efficacy of nonreactive low molecular weight antimicrobial agents on biofilm cells may not necessarily be caused by diffusion resistance.

The research was supported by the cooperative agreement EED-8907039 between the National Science Foundation and Montana State University. The authors thank James D. Bryers and Gill G. Geesey for their valuable advise and discussions and Peg Dirckx for providing the graphics.

NOMENCLATURE

a	diameter of initial sphere m
C_o	initial concentration mol/m^3
C_r	concentration at radius r mol/m^3
D	diffusion coefficient m^2/s
D_e	effective diffusion coefficient m^2/s
D_w	diffusion coefficient in water m^2/s
D_c	diffusion coefficient in cell clusters m^2/s
D_v	diffusion coefficient in biofilm voids m^2/s
k_B	Boltzmann constant J/K
MW	molecular weight g/mol
r	radius m
R_a	molecular radius diffusing compound m
R_f	radius polymer fiber m
R_p	pore radius in polymer gel m
t	time s
T	temperature K
ϵ	porosity—
η	viscosity Pa.s
τ	tortuosity—
φ_p	polymer volume fraction—

References

Anwar, H., Strap, J. L., Costerton, J. W. 1992. Kinetic interaction of biofilm cells of *Staphylococcus aureus* with cephalexin and tobramycin in a chemostat system. Antimicrob. Agents Chemother **36**: 890–893.

Arnold, F. H., Blanch, H. W., Wilke, C. R. 1985. Analysis of affinity separations II: The characterization of affinity columns by pulse techniques. Chem. Eng. J. **30**: B25–36.

Axelrod, D., Koppel, D. E., Schlesinger, J., Elson, E. and Webb, W. W. 1976. Mobility measurement by analysis of fluorescence photobleaching recovery kinetics. Biophys. J. **16**: 1055–1069.

de Beer, D., Srinivasan, R., Stewart P. (1994a) Direct measurement of chlorine penetration into biofilms during disinfection. Appl. Environm. Microbiol. **60(12)**: 4339–4344.

de Beer, D., Stoodley, P., Roe, F., Lewandowski, Z. 1994b. Effects of biofilm structure on oxygen distribution and mass transport. Biotechnol. Bioeng. **43**: 1131–1138.

de Beer, D., Stoodley, P., Lewandowski, Z. 1994c. Liquid flow in heterogeneous biofilms. Biotechnol Bioeng. **44(5)**: 636–641.

Berg, H. C. 1983. Random walks in biology. Princeton University Press.

Blonk, C. G., Don, A., Van Aalst, H., Birmingham, J. J. 1993. Fluorescence photobleaching recovery in the confocal scanning light microscope. J. Microscopy **169**: 363–374.

Boyer, M. B., Hsu, J. T. 1992. Experimental studies of restricted protein diffusion in an agarose matrix. AIChE J. **38**: 259–272.

Brenner, H., Gaydos, L. J. 1977. The constrained brownian movement of spherical particles in cylindrical pores of compatible radius. J. Coll. Interfac. Sci. **58**: 312–356.

Brown, M. R. W., Allison, D. G., Gilbert, G. 1988. Resistance of bacterial

biofilms to antibiotics: a growth-rate related effect? J. Antimicrob. Chemother. **22**: 777–780.

Christensen, B. E., Characklis, W. G. 1990. Physical and chemical properties of biofilms, p. 93–130. In: Characklis, W. G., Marshall, K. C., (eds.), Biofilms. John Wiley & Sons, New York.

Costerton, J. W., Cheng, K. J., Geesey, G. G., Ladd, T. I., Nickel, J. C., Dasgupta, M., Marrie, T. J. 1987. Bacterial biofilms in nature and disease. Ann. Rev. Microbiol. **41**: 435–464.

Crank, J. 1975. The mathematics of diffusion, p 27. 2nd ed. Oxford University Press, Oxford.

Eng, R. H. K., Padberg, F. T., Smith, S. M., Tan, E. N., Cherubin, C. E. 1991. Bactericidal effects of antibiotics on slowly growing and nongrowing bacteria. Antimicrob. Agents Chemother. **35**: 1824–1828.

Glazer, A. N. 1988. Phycobiliproteins. Meth. Enzymol. **167**: 291–303.

Griebe, T., Chen, C., Srinivasan, R., Stewart, P. S. 1994. Analysis of biofilm disinfection by free monochloramine and free chlorine, p. 151–161. In: G. G. Geesey, Z. Lewandowski, H.-C. Flemming (eds.) Biofouling/biocorrosion in industrial systems. Lewis, Chelsea.

Lawrence, J. R., Korber, D. R., Hoyle B. D., Costerton, J. W., and Caldwell, D. E. (1991) Optical sectioning of microbial biofilms. *J. Bacteriol.* **173**: 6558–6567.

Libicki, S. B., Salmon, P. M., Robertson, C. R. 1988. The effective diffusive permeability of a nonreacting solute in microbial cell aggregates. Biotechnol. Bioeng. **32**: 68–85.

Marrie, T. J., Harding, G. K. M., Ronald, A. R., Dikkema, K., Lam, J., Hoban, S., Costerton, J. W. 1979. Influence of mucoidy on antibody coating of *Pseudomonas aeruginosa.* J. Infect. Dis. **139**: 357–361.

Massol-Deya A. A., Whallon, J., Hickey, R. F., and Tiedje, J. M. (1994) Channel structures in aerobic biofilms of fixed-film reactors treating contaminated groundwater. *Appl. Environ. Microbiol.* **61(2)**: 769–777.

Muhr, A. H., Blanshard, J. M. V. 1982. Diffusion in gels. Polymer **23**: 1012–1026.

Nichols, W. W., Evans, M. J., Slack, M. P. E., Walmsley, H. L. 1989. The penetration of antibiotics of mucoid and non-mucoid *Pseudomonas aeruginosa.* J. Gen. Microbiol. **135**: 1291–1303.

Nugent, L. J., Jain, R. K. 1984. Extravascular diffusion in normal and neoplastic tissues. Cancer Res **44**: 238–244.

Radomsky, M. L., Whaley, K. J., Cone, R. A., Saltzman, W. M. 1990. Macromolecules released from polymers: diffusion into unstirred fluids. Biomaterials **11**: 619–624.

Rodbard, D., Chranbach, A. 1970. Unified theory for gel electrophoresis and gel filtration. Proc. Nat. Acad. Sci. **65**: 970–977.

Rudd, J. W. M., Kelly, C. A., St Louis, C. A., Hesslein, R. H., Furutani, A., Holoka, M. H. 1986. Microbial consumption of nitric acids in acidified north temperate lakes. Limnol. Oceanogr. **31**: 1267–1280.

Satterfield, C. N., Colton, C. K., Pitcher, Jr, W. H. 1973. Restricted diffusion in liquids within fine pores. AIChE J. **19**: 628–635.

Siebel, M., Characklis, W. G. 1991. Observations of binary population biofilms. Biotechnol. Bioeng. **37**: 778–789.

Siegrist, H., Gujer, W. 1985. Mass transfer mechanisms in a heterotrophic biofilm. Wat. Res. **19**: 1369–1378.

Treybal, R. E. 1981. Mass transfer operations. 3th edition, McGraw-Hill, pp 33–35.

Waki, S., Harvey, J. D., Bellamy, A. R. 1982. Study of agarose gels by electron microscopy of freeze-fractured surfaces. Biopolymers **21**: 1909–1926.

Westrin, B. E. 1991. Diffusion measurements in gels. PhD thesis, Dept. Chemical Engineering, Lund University.

Young, M. E., Carroad, P. A., Bell, R. L. 1980. Estimation of diffusion coefficients of proteins. Biotechnol. Bioeng. **22**: 947–955.